

NASA Technical Memorandum 100131

# Overview of Heat Transfer and Fluid Flow Problem Areas Encountered in Stirling Engine Modeling

(NASA-TM-100131) OVERVIEW OF HEAT TRANSFER  
AND FLUID FLOW PROBLEM AREAS ENCOUNTERED IN  
STIRLING ENGINE MODELING (NASA) 23 p  
CSCL 10B

N88-17561

G3/85 Unclas  
0124539

Roy C. Tew, Jr.  
*Lewis Research Center*  
*Cleveland, Ohio*

February 1988

**NASA**

OVERVIEW OF HEAT TRANSFER AND FLUID FLOW PROBLEM AREAS ENCOUNTERED IN  
STIRLING ENGINE MODELING

Roy C. Tew, Jr.  
National Aeronautics and Space Administration  
Lewis Research Center  
Cleveland, Ohio 44135

SUMMARY

NASA Lewis Research Center has been managing Stirling engine development programs for over a decade. In addition to contractual programs, this work has included in-house engine testing and development of engine computer models. Attempts to validate Stirling engine computer models with test data have demonstrated that engine thermodynamic losses need better characterization. Various Stirling engine thermodynamic losses and efforts that are underway to characterize these losses are discussed.

NOMENCLATURE

$A_R$	ratio of fluid displacement to heat exchanger length; also, $A_R = L Re_{max}/(2D Re_\omega)$
$D$	characteristic diameter
$L$	heat exchanger length
$Q_C$	energy flux per cycle from cooler
$Q_H$	energy flux per cycle to heater
$Q_{REG}$	regenerator energy flux loss per cycle
$Q_{WASTE}$	energy flux per cycle from compression space to cooler
$W_{EXP}$	work per cycle done by expansion space gas on displacer
$W_{PISTON}$	power piston work per cycle
$Re_{max}$	Reynolds number based on maximum cross-sectional mean velocity
$Re_\omega = \omega D^2/4\nu$	dimensionless frequency or oscillating flow Reynolds no. or Valensi number
$T_{cold}$	engine cold end or cooler temperature
$T_{hot}$	engine hot end or heater temperature
$T_{ratio}$	$T_{hot}/T_{cold}$

Greek:

- $\nu$                     kinematic viscosity  
 $\omega$                     frequency, rad/sec

## INTRODUCTION

NASA Lewis began managing a Stirling engine automotive development program for the Department of Energy about 12 yr ago. The engines developed and tested in the automotive program have all been kinematic (crank drive) engines. More recently, free-piston Stirling engines have begun to be developed for space-power applications. Several kinematic and free-piston engines have been tested and modeled at NASA Lewis in support of these development efforts.

Much early use was made of code calibration in order to get engine models to agree with overall performance data. It was found that different combinations of predicted losses could yield good agreement with the data for a particular engine. As a result, a model calibrated to agree with data from one or several engines could not be reliably extrapolated to a significantly different engine. It was concluded that a number of heat transfer and fluid flow phenomena were not well characterized.

In general, the accuracy of Stirling computer models in predicting the thermodynamic performance of engines for which the models have not been calibrated, is still less than desired. When an uncalibrated model's predictions of indicated power and efficiency prove to be within 10 percent of the data, agreement is considered to be good. However, errors of 20 percent or more are common.

Partially due to thermodynamic calculation errors, Stirling engines usually require considerable hardware modification, after the first build, in order to approach their design goals. Improved characterization of engine fluid flow and heat transfer phenomena would cut the cost of engine development and permit consideration of more innovative designs.

Due to the rapid oscillations (up to 105 Hz) of gas temperatures, pressure level, pressure drops, and mass flows, it has not been possible to make direct comparisons of predicted instantaneous pressure drops and gas temperatures with data, nor to verify predictions of viscous dissipation or heat transfer rates. Reasons for this have been the lack of measurement techniques for making "in engine" measurements at Stirling engine frequencies and the lack of specialized test rigs.

As a result of engine measurements, steady-flow testing, and analysis it has been possible to list thermodynamic loss mechanisms (or concentrations of irreversibilities) that are thought to include all of the major thermodynamic losses. These loss mechanisms are discussed briefly. A Stirling engine "loss understanding" effort is underway. The main thrust of this effort is to characterize the various thermodynamic losses by (1) use of specialized test rigs which can isolate the effects of various phenomena, (2) using improved engine and rig instrumentation to make dynamic measurements, and (3) development of

multidimensional simulations to be used in combination with engines and test rigs to characterize multidimensional effects. Several components of the effort are discussed.

#### CHARACTERISTICS OF THE STIRLING ENGINE THERMODYNAMIC ENVIRONMENT

Stirling engines typically contain hydrogen, helium or air in a closed "working space." They are reciprocating engines which contain three different heat exchangers in series--a heater, regenerator and cooler--within the working space. A schematic of a Stirling engine is shown in figure 1. The schematic depicts a single-cylinder "free-piston" displacer-power piston engine; in such engines the piston motions are controlled by use of gas springs. Electrical power can be removed by connecting the power piston to a linear alternator. Hydraulic or pneumatic power may also be removed by use of appropriate piston and load configurations. The displacer and piston can, alternatively, be linked to a mechanical crank as in "kinematic" engines.

The function of the displacer is to cycle the gas between the hot expansion space and the cold compression space through the three heat exchangers; its motion is usually close to sinusoidal. The power piston alternately compresses and expands the gas; its almost sinusoidal motion lags that of the displacer. When (1) compression volume variation lags that of the expansion volume by the appropriate amount, (2) heater, regenerator, and cooler perform satisfactorily, and (3) other engine losses are not too large, then expansion work exceeds compression work and net work is done by the gas on the power piston.

Inside the working space components, the flow oscillates about a zero mean. The engine pressure in each component oscillates about the engine mean pressure. The spatial pressure drop across the heat exchangers is smaller and less "sinusoidal" compared to the pressure variations which occur over the engine cycle. Working gas temperature also oscillates with significant amplitude, except in the regenerator; the regenerator processes are closer to isothermal than any other component. Temperature variations are largest in spaces, such as the expansion and compression spaces, where gas-to-wall heat transfer is relatively small. Nearly sinusoidal variations of the internal engine variables are characteristic of most Stirling engines. Plots of calculated P-40 engine variables can be found in reference 1.

The regenerator experiences large axial temperature gradients. For one engine, an approximately 250 K temperature drop occurs across a 2.5 cm long regenerator matrix. The regenerator acts as a thermal storage element, alternately absorbing energy from hot gas flowing in from the heater and giving it up to lower-temperature gas flowing in from the cooler. It acts as a heat "dam" to restrict heat loss directly from the heater to the cooler. Fluid "particles" in the regenerator usually do not traverse its entire length.

One free-piston engine, has been tested at a frequency in excess of 100 Hz. Many engines have been tested with mean pressures of 15 MPa (2175 psia) and a new engine is being designed for a mean pressure of 18.5 MPa (2682 psia). Maximum to minimum pressure ratios vary from about 1.2 for free-piston engines to about 1.8 for kinematic designs.

## EXAMPLES OF STIRLING ENGINE GEOMETRIES

Three engine designs will be briefly discussed. The MOD-II Automotive Stirling Engine (ref. 2) and the free-piston Space Power Demonstrator Engine or SPDE (refs. 3 to 6) are being tested. The Stirling Space Engine or SSE (refs. 3 to 6) is a conceptual design for an advanced free-piston engine.

A schematic of the MOD-II is shown in figure 2. It is a four-cylinder engine with double-acting pistons. The double-acting feature is achieved by connecting the hot-space, over one piston, via a heater, regenerator and cooler, to the cold-space under an adjacent piston. Thus each piston is in contact with two separate working spaces; the motion of each piston lags by  $90^\circ$  that of one of the adjacent pistons, and leads by  $90^\circ$  that of the other adjacent piston. Mechanical power is removed from the engine via linkages to a crankshaft. The gas flow path includes complex expansion space-heater and heater-regenerator manifolds (as a result of automobile packaging requirements). Much effort went into the design of the manifolds to try to minimize performance degradation due to flow maldistributions and other losses. A heater, regenerator and cooler are located in an annulus around each cylinder. In both the heater and the cooler, the working space gas flows through many small tubes. The heater tubes receive heat from a fossil-fuel fired combustor. The cooler tubes are in contact with a coolant mixture of water and glycol. The regenerator contains a matrix consisting of many layers of fine wire screen (a much larger heat transfer surface-to-volume ratio is required in the regenerator, compared to the heater and cooler, because much larger heat transfer rates are required for good engine performance). Hydrogen gas is used in the working space.

Operating characteristics of the MOD II are shown in table I. Design goals (ref. 2) are compared with recent measured performance (ref. 7) for two operating points. The automotive application requires that the engine operate over a wide range of conditions from idle to full load. Measured indicated power and efficiency are seen to be within about 7 percent of the design goals for both operating points. The low load point is closer to the average operating point of the engine over the combined (highway and urban) driving cycle; it is, therefore, more indicative of the engine fuel economy over this cycle. For the low load point, the measured net efficiency was low by 17 percent due largely to higher auxiliary power requirements and mechanical friction; indicated efficiency for this point was low by only about 7 percent.

A schematic of one-half of the SPDE is shown in figure 3. Two of these, nominally 12.5 kWe, modules fit together end to end with interconnected hot spaces, to provide dynamic balancing. Heat is supplied to the heater by a molten salt system in the test unit. Waste heat was removed from the cooler of the test unit by a water-glycol mixture.

The SPDE was the first free-piston engine designed to demonstrate technology for potential use in space. It has demonstrated the feasibility of producing about 14 kW of indicated power per cylinder from a free-piston design. At 105 Hz, it is the highest frequency Stirling engine ever designed. Helium gas is used in the SPDE working space.

Design and achieved operating characteristics of the SPDE are shown in table II. Achieved power is 13.5 percent lower than the design goal and achieved PV efficiency is about 45 percent lower. Since the preliminary design

of the SPDE was completed a major upgrade of the engine design code has taken place. A revised solution of the basic gas energy equation was found necessary to correct discrepancies between predictions and data observed as engine temperature ratios were reduced. It has been reported that the code predictions now match SPDE engine performance data within 10 percent with no code calibration required (ref. 8).

The SPDE engine has now been divided into two engines. These two Space Power Research Engines (SPRE) will be used for research purposes. One will be tested at Mechanical Technology, Inc. and the other will be tested at NASA Lewis.

A schematic of the SSE is shown in figure 4. At present only a conceptual design exists. (It represents the first attempt to completely optimize a free-piston design for a space-power application. The one-cylinder engine is designed to produce 25 kW of electrical power. An active dynamic balancing unit is included.) A unique feature is the modularized unit that includes a heat pipe heater, a regenerator and a cooler. About 40 of these modularized units should be adequate; this contrasts with the approximately 1600 heater and 1600 cooler tubes per cylinder in the SPDE. The SSE was also designed for use with helium gas. SSE operating characteristics are shown in table III. Engine frequency is somewhat lower than that of the SPDE, but mean pressure and pressure amplitude are both higher.

Free-piston displacer and piston motions are designed by choosing appropriate gas springs to balance the masses of the reciprocating pistons. Working space pressure drops must be accounted for in sizing the displacer gas springs and the effective displacer "rod area." The working space itself is one of the springs that must be considered in the design of the dynamics. The characteristics of this working space spring are a function of piston motions, leakages from the working space and heat exchanger heat transfer characteristics. Thus both the thermodynamics and the engine dynamics are sensitive to thermodynamic losses. It follows that, in the design of free-piston engines, good loss characterization is especially important.

Several engines have been tested and modeled at NASA Lewis. They include the one-cylinder General Motors GPU-3 engine (ref. 9) the four-cylinder P-40 automotive prototype engine (refs. 1 and 10) the one-cylinder RE-1000 free-piston engine (refs. 11 and 12) and the four-cylinder Philips ADVENCO engine (ref. 13). An upgraded Mod I engine was recently used to test new seal concepts. The SPRE is to begin tests at NASA Lewis by summer 1987. Testing of the RE-1000 free-piston engine is continuing with a hydraulic load. Plans are being made to fabricate and test several SSE heat exchanger modules in an RE-1000 engine at NASA Lewis.

#### EFFECT OF TEMPERATURE RATIO ON THE SENSITIVITY OF ENGINE PERFORMANCE TO THERMODYNAMIC LOSSES

The Mod II Automotive Stirling Engines was designed for a temperature ratio,  $T_{ratio}$ , of about 3.4 (table I). The new space-power free-piston engines are being designed for  $T_{ratio} = 2$  (tables II and III); the low temperature ratios permit higher cold-end temperatures so that the waste heat radiators will be smaller. Figure 5 shows the sensitivity of a conceptual SSE engine design (designed for  $T_{ratio} = 2$ ) to changes in heater and cooler heat

transfer coefficients at  $T_{ratio} = 2$  and 3 (ref. 14). It is seen that engine performance is more sensitive to heater and cooler heat transfer rates at  $T_{ratio} = 2$ . Consequently, engine efficiency is expected to be more sensitive to losses of all kinds for the new space power designs. It is, therefore, more essential for all important losses to be well characterized.

#### DISCUSSION OF HEAT TRANSFER AND FLUID FLOW PROBLEM AREAS IN STIRLING ENGINE MODELING AND DESIGN

Figure 1 indicates various fluid flow and heat transfer problem areas. These are:

(1) Instantaneous heat transfer rates between gas and metal in the heat exchangers. Accurate average heat transfer rates are not sufficient. The heat transfer rate at a particular position varies periodically over the cycle and engine performance is sensitive to the phasing of these variations.

(2) Instantaneous heat transfer rates in regions where the surface-to-volume-ratio is relatively small (which lead to hysteresis losses). Heat transfer rates in regions with small surface-to-volume-ratios, such as gas springs, expansion and compression spaces, and connecting ducts are important. Hysteresis losses are zero in these spaces if the processes occurring there are isothermal or adiabatic. For processes which are neither isothermal nor adiabatic, however, hysteresis losses can be large.

(3) Instantaneous pressure drop across the displacer and the amount of viscous dissipation over the cycle. For the SPDE engine, preliminary design calculations indicated that the magnitude of the pressure drop due to gas inertia was about the same as the pressure drop due to wall shear stress (ref. 15). Knowledge of the magnitude and phasing of the total pressure drop across the displacer is important in calculating the dynamics of an engine. Viscous dissipation is an important part of the engine thermodynamic loss.

(4) End-effects heat transfer and pressure drop. These effects must be considered wherever significant area transitions occur.

(5) Net energy flux through the regenerator from the heater to the cooler. This flux is a short circuit of heat directly to the cooler. Enhanced axial thermal conductivities may need to be assumed in design codes to account for (1) limitations of one-dimensional models and (2) the effects of eddies in turbulent flow through the matrix.

(6) Flow maldistributions. The one-dimensional codes used for engine modeling assume that the flow profile is identical in each of the heater and cooler tubes. The flow is also assumed to be uniform, radially, across the regenerator matrix. Characterizations of losses due to flow maldistributions need to be developed for use in design codes.

(7) Appendix gap losses. A very complex loss occurs in the annular gap, or "appendix gap," between the displacer and the cylinder.

(8) "Adiabatic" losses. Irreversible thermodynamic losses occur when elements of gas at different temperatures are mixed together and when heat flows across a temperature difference between the metal wall and the gas.

When small-surface-to-volume-ratio regions (which tend to be closer to adiabatic than isothermal) are adjacent to nearly isothermal heat exchangers, these losses are enhanced.

Although no definitive information about the relative magnitudes of these losses is available, SPDE preliminary design calculations (ref. 15) give some information. Table IV shows a thermodynamic loss breakdown for one cylinder of the SPDE. Flow maldistribution effects were not accounted for and "adiabatic" losses are not separated, as such, from other losses. Working space losses related to heat transfer are seen to be important, as indicated by the sum of working space "hysteresis" and "loss due to heater and cooler gas-to-wall temperature difference." Working fluid pumping is also an important power loss. The total of the gas spring power losses is also significant. Leakage losses, though shown to be small here, not may be precisely predictable for untested geometrical clearances under oscillating, flow conditions. Direct thermal losses, ranked according to the magnitude of the calculations, are regenerator energy flux, conduction, and appendix gap losses (relative magnitudes could be different for different designs). Regenerator energy flux and appendix gap losses can, if sufficiently large, cause a degradation in power in addition to increased heat input.

#### Heat Transfer Rates, Pressure Drop, Wall Shear Stress and Viscous Dissipation in Stirling Engine Heat Exchangers

Steady-flow heat transfer and friction factor correlations are being used in most one-dimensional flow Stirling performance and design codes; correlations from reference 16 are frequently used. Laminar flow theory exists for predicting how flow oscillations affect viscous dissipation and pressure drop. However, according to one-dimensional flow calculations, heater and cooler flow regimes are primarily turbulent for many engine designs (according to steady-flow turbulent criteria). No theory exists for predicting the effect of flow oscillations on viscous dissipation and pressure drop, in the turbulent regime, or on heat transfer rates in either laminar or turbulent regimes.

Seume and Simon have summarized what is known about the effects of oscillating flow on heat transfer, wall shear stress, viscous dissipation and pressure drop (refs. 17 and 18). Similarity parameters proposed to characterize these effects are  $RE_{max}$ ,  $Re_{\omega}$  and  $A_R$  or  $L/D$ . Since Mach number are calculated to be less than 0.1 for most designs, acoustic effects are thought to be small (density does, however, vary significantly with position due to large axial temperature gradients and with time due to large variations in pressure level over the cycle). Calculations were made with a Schmidt model for many different Stirling engines. Resulting plots of the similarity parameters for the heaters, regenerators and coolers of these engines are given in reference 18. It was concluded that more research was needed to understand the process of transition and the effect of flow oscillation on turbulent momentum and heat transfer.

Seume and Simon have constructed a test rig to do the research they recommended. A schematic of the rig is shown in figure 6. The working fluid will be air. Two relatively large diameter test sections will permit measurements of multidimensional profiles using hot wire anemometers. The relatively low maximum frequency, about 400 rpm, should allow accurate dynamic measurements of pressure, velocity and temperature. A recent description of their

planned test program (ref. 19) indicates rig qualification tests are planned for the summer of 1987. A discussion of what Simon and Seume consider to be the unresolved issues in tube and matrix flow oscillation effects is given in reference 20.

Wood has designed and built an oscillating flow rig to be used in measuring pressure drops through tubes and matrices at engine design frequencies (ref. 21); this rig is to be used to develop correlations for use in one-dimension models. A schematic of the rig is shown in figure 7. A linear motor is used to drive the rig at frequencies up to 120 Hz. Different sets of springs are used in different frequency ranges, to reduce the drive power requirements. The initial rig is designed to test for effects of oscillating flow only (pressure level will be essentially constant). However, another drive can be added to test for the combined effects of oscillating flow and pressure level. A unidirectional flow rig has also been constructed so that the same heat exchanger geometries can be tested under both steady-flow and oscillating-flow conditions. A schematic of this rig is shown in figure 8.

One early set of oscillating flow rig data taken during checkout of the rig and data system, is shown in figure 9 (ref. 22). Dynamic pressure is shown over a cycle for a frequency of 28 Hz. Also shown are Fast Fourier Transforms of the pressure drop and piston motion data. The magnitude of the third harmonic for the pressure drop was larger than anticipated, based on previous calculations.

Figure 5 shows how sensitive conceptual SSE design performance was to heater and cooler heat transfer coefficients. Penswick has suggested that heat transfer coefficients may be lower than predicted by steady-flow correlations (ref. 14).

#### Heat Transfer Rates in Small-Surface-to-Volume-Ratio Regions and Hysteresis Losses

Hysteresis losses are a major concern in the design of gas springs and are also thought to be important in expansion and compression spaces, and in connection ducts. Hysteresis losses are zero in a gas spring if the process is adiabatic or isothermal. For a process which is neither isothermal nor adiabatic, the net heat transfer per cycle from gas to wall is equivalent to a loss of useful work or a hysteresis loss. Hysteresis losses become more important as engine frequency increases. The thermodynamic loss breakdown in table IV for the preliminary SPDE design calculations shows working-space plus gas-spring hysteresis losses equivalent to 15.4 percent of the indicated power or 2.35 kW.

Figure 10 shows how calculated SSE design power varies with the relative heat transfer rates in expansion and compression spaces and associated gas manifolds (ref. 14). The figure suggests that, if the heat transfer rate could be reduced from the reference value to zero, then the power would increase by about 3 kW or 8 percent; this implies a reference hysteresis loss of about 3 kW in expansion and compression spaces and associated manifolds (this does not include hysteresis losses in the gas springs). Penswick's discussion of the accuracy of the current heat transfer rates calculated for the expansion and compression spaces and their manifolds, suggests that the reference hysteresis loss could be in error by a factor as large as 2.

In an early engine design, Kangpil Lee concluded that hysteresis losses were a major thermodynamic loss in the engine (ref. 23). Figure 11 (ref. 24) shows how hysteresis losses were calculated to vary in the RE-1000 free-piston engine as the expansion and compression space heat transfer coefficients were varied between an isothermal and adiabatic process. This result suggests that the hysteresis loss can become large in expansion and compression spaces.

Closed form expressions for calculating hysteresis losses have been developed (ref. 25). These equations help understand how hysteresis losses vary with various engine parameters' and are useful in estimating hysteresis losses for closed volume gas springs.

Faulkner and Smith (ref. 26) have shown experimentally that the phase lag between cylinder heat transfer and wall-to-average-gas temperature difference varied from 0° for isothermal to 90° for adiabatic processes. Analytical expressions for the magnitude and phase lag of cylinder heat transfer have been derived by Lee (ref. 23) and others (ref. 27). Kornhauser and Smith have tested a gas spring and have reported the results of using various cylinder heat transfer correlations and hysteresis loss equations to predict hysteresis losses for comparison with their test data (ref. 27).

The characterization of "open volume" hysteresis heat transfer may prove to be significantly different than that for a "closed volume" gas spring, due to the inflow and outflow of gas that occurs in an open volume. In the expansion space of a Stirling engine, for example, gas flow depends more on displacer motion than on piston motion and pressure level depends more on piston motion than on displacer motion. Since piston motion lags that of the displacer by a substantial amount in an engine, the phasing between gas flow and pressure is different than in a gas spring.

#### Heat Transfer and Pressure Drop End Effects

Seume and Simon calculated, based on steady unidirectional turbulent flow in a rough pipe, that between 15 and 50 percent of the heater and cooler pressure drops occurred at the pipe entrance and exits in the engines they modeled (ref. 18). For the SPDE the value they calculated was about 35 percent for heater and cooler. They also estimated that developing velocity profiles may be expected throughout many heaters and coolers over the engine cycle. One conclusion of their initial grant was that more research is needed on the effects of thermal and hydrodynamic entrance lengths on heat transfer and pressure drop.

#### Net Energy Flux Through the Regenerator

As noted earlier, this flux is a short circuit of heat through the regenerator, directly to the cooler. An increase in this flux will cause some combination of an increase in heat input and a decrease in engine power. This can be seen by reference to figure 12, where the energy fluxes shown are net values over the cycle (fig. 12 ignores hysteresis losses in expansion and compression spaces and displacer power requirements).

Suppose the energy stored in the regenerator per 1/2 cycle is 5 times the net heat into the engine per cycle (a reasonable assumption, according to

calculations). Then a 1 percent decrease in energy stored in the matrix (and a corresponding increase in regenerator energy flux loss) causes a 5 percent increase in heat input to the heater (assuming adequate heater capacity) and a 5 percent decrease in efficiency. If the heater capacity is not adequate to make up the additional regenerator energy flux loss, then power will drop and the loss of engine efficiency will be even greater.

Gedeon has shown (ref. 28) that regenerator flux losses may be underestimated due to limitations of one-dimensional Stirling models in predicting oscillating-flow phenomena. Edwards and Richardson (ref. 29) demonstrated enhancements in the dispersion of argon gas through air with increases in the steady-flow Reynolds no. (presumably due to eddy diffusion). Gedeon has suggested (ref. 30) that, by analogy, Edwards and Richardson's experiment argues for enhancements in effective gas thermal conductivity with increases in the steady-flow Reynolds number. A grant has been awarded to Professor Alexander Dybbs of Case Western Reserve University to investigate effective thermal conductivities in porous matrices under conditions approximating those in a Stirling engine.

Ziph has described a test rig that was developed by N.V. Philips to characterize regenerator flux losses empirically (ref. 31). By testing a matrix in this oscillating flow rig, it is possible to generate an empirical expression for regenerator flux loss as a function of a set of dimensionless parameters (equivalent to those recommended by Simon and Seume). This test rig has been transported to the U.S. Regenerator data taken with this rig could be used to evaluate the regenerator models used in Stirling design and performance codes.

#### Flow Maldistributions

The one-dimensional codes used for engine modeling and design assume that the flow profile is identical in each parallel tube and is uniform across the regenerator matrix. However, measurements of tube-to-tube temperature differences in an automotive Stirling engine heater head (ref. 8) suggested that there were substantial differences in flow from tube-to-tube. Use of a general fluid flow code, PHOENICS, to calculate steady two-dimensional flow from the SPDE heater tubes into the regenerator matrix, initially caused concern that jetting into the matrix might be causing significant pressure drop (ref. 32). However, later analysis of an experimental displacer force phasor diagram led to conclusions that pressure drop across the displacer had been less than predicted with steady-flow correlations (ref. 33).

Gedeon is developing a two-dimensional periodic flow model (ref. 34) to study manifold-regenerator oscillating flows. A prototype version of the code was used to generate figure 13. Figure 13 shows that in a side-inlet manifold design, where pressure drop across the matrix was of the same order of magnitude as that through the manifolds, the flow distribution through the matrix was calculated to be very nonuniform. When the pressure drop across the matrix was increased by a factor of 50, while the manifold pressure drop remained about the same, the flow was much more uniform (shown in fig. 14).

The space-power Stirling designs, with  $T_{ratio} = 2$ , tend to have shorter regenerator lengths than designs with higher temperature ratios. The resulting

smaller ratios of regenerator-to-manifold pressure drop increase the risk of flow maldistributions in the regenerator.

Multidimensional measurements of velocities are to be made in the oscillating flow tests to be run by Seume and Simon (ref. 19). A two-dimensional engine code under development by Goldberg (ref. 35) may be used in conjunction with these tests. In particular, Goldberg hopes to test the prediction of various turbulence models against the test results of Seume and Simon. Goldberg believes that two-dimensional effects may be of major importance in the expansion and compression spaces of the SPDE. In particular, the expansion-space flow field could have a significant impact on the flow distribution among the heater tubes.

### Appendix Gap Losses

The appendix gap is the annular volume between the hot end of the displacer and the cylinder wall. The complex fluid flow and heat transfer phenomena which take place in the gap involve several irreversibilities which degrade the performance of the engine.

Huang has developed a detailed appendix gap model (refs. 36 to 38). Three heat loss mechanisms are modeled: (1) axial conduction along the piston and cylinder, (2) radial heat transfer between the gas in the gap and the boundary walls, and (3) leakage enthalpy flow across the cold end seal. The radial heat transfer mechanism is the most complicated and least understood; it can be subdivided into a pure conduction or "shuttle" component and a complicated convection component which is commonly identified as the appendix gap "pumping" loss.

Appendix gap losses have proved difficult to determine accurately from engine test data. A loss of about 6.3 kW was calculated for the upgraded MOD-I automotive Stirling engine at full load with Huang's model (ref. 37). The calculated loss of 6.3 kW is 3.6 percent of the measured 175 kW of heat into the engine (ref. 39). Since the space engine designs have smaller pressure and temperatures ratios than the automotive engines, appendix gap loss should be of less importance in the space engines. Table IV shows that the appendix gap loss calculated for the preliminary design of the SPDE was 1.33 kW per cylinder or 2.7 percent of the heat input per cylinder.

### Adiabatic Losses

Chen et. al., (ref. 24) give an explanation of "adiabatic" losses (or losses that are caused by adiabatic or near-adiabatic volumes in the Stirling engine working space). Three components of the calculated RE-1000 engine loss are shown in figure 11 as functions of cylinder heat transfer coefficients. The first component is the hysteresis loss discussed earlier. The second and third components are "adiabatic" losses or components of the loss for adiabatic cylinder processes (the hysteresis loss is zero for an adiabatic process). One "adiabatic" loss component, the "external heat transfer", is caused by gas leaving the cylinder (expansion or compression space) and entering the adjacent heat exchanger at a significantly different temperature than the walls of the exchanger. The other adiabatic loss component is the mixing loss caused by gas from an adjacent heat exchanger entering the cylinder and mixing with its gas. Figure 11 suggests that attempts to isothermalize the cylinder of the RE-1000 would reduce the net "adiabatic" losses but might produce a net decrease in

performance due to increased hysteresis loss. Large nearly-adiabatic connecting duct volumes are especially undesirable between heater-regenerator and regenerator-cooler, where the external heat transfer and mixing losses would occur for both flow directions.

#### CONCLUDING REMARKS

The new free-piston Stirling engines for space power are being designed for low-temperature ratios. Engine performance for low-temperature-ratio designs is more sensitive to losses of all kinds.

The predicted performance of Stirling engine designs for space power is especially sensitive to the heat transfer rates between gas and metal in all engine components, and the pressure drop across the heat exchanger components (and thus the displacer). Steady-flow heat transfer and friction factor correlations are being used in one-dimensional Stirling models. Effects of oscillating flow on heat transfer and pressure drop for Stirling engine operating conditions are not known. Effects of flow maldistributions (or deviations from the one-dimensional flow assumptions used in design codes) are not known, although design practice is to try to minimize such maldistributions. The effects of area transition or "end effects" on heat transfer and pressure drop in an oscillating-flow environment are also not understood. Huang's detailed computer model of an appendix gap has not been adequately verified with test data. Leakage losses are also a significant concern.

Several test programs aimed at characterizing heat transfer rates and pressure drop effects in Stirling engine components under Stirling engine operating conditions are getting underway. These efforts are reasonably low cost compared to engine hardware development programs, but require a sustained effort over several years to produce conclusive results. These efforts should be sustained until engine thermodynamic design becomes so routine that it is clear that heat transfer rate and pressure drop effects have been adequately characterized.

#### REFERENCES

1. Tew, R.G., Jr.: Computer Program for Stirling Engine Performance Calculations Final Report: NASA TM-82960, 1983.
2. Nightingale, N.P.: Automotive Stirling Engine: Mod 2 Design Report. NASA CR-175106, 1986.
3. Alger, D.L.: Overview of the 1986 Free-Piston Stirling Activities at NASA Lewis Research Center: NASA TM-88895, 1986.
4. Slaby, J.G.: Overview of the 1986 Free-Piston Stirling SP-100 Activities at the NASA Lewis Research Center. NASA TM-87305, In: IECEC '86; Proceedings of the 21st Intersociety Energy Conversion Engineering Conference, San Diego, CA, August 25-29, 1986, Vol. 1, pp. 420-429.
5. Slaby, J.G.: Overview of Free-Piston Stirling Engine Technology for Space Power Application. NASA TM-88886, DOE/NASA/1005-12, 1987.

6. Slaby, J.G.; and Alger, D.L.: A 1987 Overview of Free-Piston Stirling Technology for Space Power Application: NASA TM-89832, In: IECEC '87; Proceedings of the 22nd Intersociety Energy Conversion Engineering Conference, Philadelphia, PA, August 10-14, 1987, Vol. 3, pp. 1371-1377.
7. Berggren, R.: Mechanical Technology, Inc., Latham, NY: Private Communication, Apr. 1987.
8. Mechanical Technology, Inc., Latham, NY: Private Communication, 1987.
9. Thieme, L.G.; and Tew, R.C., Jr.: Baseline Performance of the GPU 3 Stirling Engine. NASA TM-79038, DOE/NASA/1040-78/5, 1978.
10. Allen, D.; and Cairelli, J.: Test Results of a 40 kW Stirling Engine and Comparison with the NASA-Lewis Computer Code Predictions. In: IECEC '85; Proceedings of the 20th Intersociety Energy Conversion Engineering Conference, Miami Beach, FL, August 18-23, 1985, Vol. 3, pp. 3.238-3.243.
11. Schreiber, J.G.; Geng, S.M.; and Lorenz, G.V.: RE-1000 Free-Piston Stirling Engine Sensitivity Test Results. NASA TM-88846, 1986.
12. Geng, S.M.: Calibration and Comparison of the NASA Lewis Free-Piston Stirling Engine Model Predictions with RE-1000 Test Data," NASA TM-89853 In: IECEC '87; Proceedings of the 22nd Intersociety Energy Conversion Engineering Conference, Philadelphia, PA, August 10-14, 1987, Vol. 4, pp. 1774-1785.
13. Thieme, L.G.; and Allen, D.J.: Testing of a Variable-Stroke Stirling Engine. In: IECEC '86; Proceedings of the 21st Intersociety Energy Conversion Engineering Conference, San Diego, CA, August 25-29, 1986, Vol. 1, pp. 57-462.
14. Penswick, B.: Monthly Technical Report (under NASA Contract NAS3-23885), Sunpower, Inc., March 1987.
15. Space Power Demonstration Engine Preliminary Design Review. Mechanical Technology, Inc., May 1984.
16. Kays, W.M.; and London, A.L.: Compact Heat Exchangers, 2nd Edition, McGraw-Hill, 1964.
17. Seume, J.R.; and Simon, T.W.: Oscillating Flow in Stirling Engine Heat Exchangers. In: IECEC '86; Proceedings of the 21st Intersociety Energy Conversion Engineering Conference, San Diego, CA, August 25-29, 1986, Vol. 1, pp. 533-538.
18. Seume, J.R.; and Simon, T.W.: A Survey of Oscillating Flow in Stirling Engine Heat Exchangers. Yearly Progress Report prepared for NASA-Lewis Research Center by Univ. of Minnesota, Heat Transfer Laboratory; NASA Grant NAG3-598, October 1986.
19. Seume, J.R.; Goldberg, L.F.; and Simon, T.W.: Description of an Oscillating Flow Test Program. In: IECEC '87; Proceedings of the 22nd Intersociety Energy Conversion Engineering Conference, Philadelphia, PA, August 10-14, 1987, Vol. 4, pp.1753-1758.

20. Seume, J.R.; and Simon, T.W.: Flow Oscillation Effects in Tubes and Porous Material Unresolved Issues. Presented at the ASME Symposium on Fluid Flow and Heat Transfer in Reciprocating Machinery, Dec. 13-18, 1987, Boston, MA.
21. The Design of a Device to Measure Reversing Flow Pressure Drops in Stirling Engine Heat Exchangers-Phase I Final Report. Sunpower Inc., NASA Contract NAS3-24396 August 1985.
22. Wood, J. Gary: Oscillating Flow Pressure Drop Test Rig. Sunpower, Inc., NASA Contract NAS3-24879, March 1987.
23. Lee, K.: A Simplistic Model of Cyclic Heat Transfer Phenomena in Closed Spaces. In: IECEC '83; Proceedings of the 18th Intersociety Energy Conversion Engineering Conference, Orlando, FL, Aug. 21-26, 1983, Vol. 2, pp. 720-723.
24. Chen, N.C.J.; Griffin, F.P.; and West, C.D.: Simplified Analysis of Stirling Engines and Heat Pumps. Oak Ridge National Laboratory Report, ORNL/TM-9498, 1985.
25. Urieli, I; and Berchowitz, D.M: Stirling Cycle Engine Analysis, Adam Hilger Ltd., 1984.
26. Faulkner, H.B.; and Smith, J.L.,: Instantaneous Heat Transfer During Compression and Expansion in Reciprocating Gas Handling Machinery. In: IECEC '83; Proceedings of the 18th Intersociety Energy Conversion Engineering Conference, Orlando, FL, Aug. 21-26, 1983, Vol. 2, pp. 724-730.
27. Kornhauser, A.A.; and Smith, J.L., Jr.: A Comparison of Cylinder Heat Transfer Expressions Based on Prediction of Gas Spring Hysteresis Loss. Presented at the ASME Symposium on Fluid Flow and Heat Transfer in Reciprocating Machinery, Dec. 13-18, 1987, Boston, MA.
28. Gedeon, D.: Mean-Parameter Modeling of Oscillating Flow. J. Heat Transfer, Vol. 108, No. 3, 1986, pp. 513-518.
29. Edwards, M.F.; and Richardson, J.F.: Gas Dispersion in Packed Beds. Chem. Eng. Sci., Vol. 23, No. 2, 1968, pp. 109-123.
30. Gedeon, D., Gedeon Associates, Athens, OH: Private Communication, May 1987.
31. Ziph, B., Stirling Thermal Motors, Inc., Ann Arbor, MI: Private Communication, Apr. 1987.
32. Sjöholm, J.: Private Communication, 1985.
33. Dahr, M.: Mechanical Technology Inc., Latham, NY: Private Communication, 1986.
34. Gedeon, D.: A Computer Program for Modeling Two-Dimensional Gas Flow in Stirling Engine Regenerators: Final Report. Prepared for NASA Lewis Research Center under Contract DEN3-308, Gedeon Associates, 1986.

35. Goldberg, L.: The Simulated Systems Impact of Two-Dimensional Oscillating Flows in a Stirling Machine Heat Exchanger. Presented at the ASME Symposium on Fluid Flow and Heat Transfer in Reciprocating Machinery, Dec. 14-16, 1987, Boston, MA.
36. Huang, S.C.: Appendix Gap Loss in Stirling Engines, Analysis and User's Manual. Mechanical Technology, Inc., NASA Contract DEN3-32, MIT-85ASE487ER79, 1985.
37. Huang, S.C.: Upgraded MOD-1 Engine Raised Appendix Gap Test/Code Correlation. Mechanical Technology, Inc., NASA Contract DEN3-32, MTI-86ASE488ER80, 1986.
38. Huang, S.C.; and Berggren, R.: Evaluation of Stirling Engine Appendix Gap Losses. In: IECEC '86; Proceedings of the 21st Intersociety Energy Conversion Engineering Conference, San Diego, CA, August 25-29, 1986, Vol. 1, pp. 562-568.
39. Foster, J.M.: Upgraded MOD-1 Engine No. 5 Acceptance Test Report. Mechanical Technology Inc., NASA Contract DEN3-32, MTI-85ASE457ER76, 1985.

TABLE I. - MOD II OPERATING CHARACTERISTICS

[ $T_{\text{hot end}} = 820 \text{ }^\circ\text{C}$  (1093 K),  $T_{\text{cold end}} = 50 \text{ }^\circ\text{C}$  (323 K),  $T_{\text{ratio}} = 3.38$ .]

(a) Full load point (mean pressure = 15 MPa (2175 psia), engine speed = 4000 rpm)

	Design	4/87 Performance in vehicle
Indicated power, kW	78.6	73.1
Indicated efficiency	35.6	33.4
Friction, kW	9.9	9.8
Auxiliaries, kW	6.4	9.0
Net power, kW	62.3	54.3
External heat system efficiency, percent	88.9	89.6
Net efficiency	28.2	24.8

(b) Low load point (mean pressure = 5 MPa (725 psia), engine speed = 1000 rpm)

	Design	4/87 Performance in vehicle
Indicated power, kW	9.1	8.9
Indicated efficiency	41.4	38.4
Friction, kW	0.9	1.1
Auxiliaries, kW	1.0	1.6
Net power, kW	7.1	6.2
External heat system efficiency, percent	88.9	85.8
Net efficiency	32.3	26.8

TABLE II. - SPACE POWER DEMONSTRATOR ENGINE (SPDE)  
OPERATING CHARACTERISTICS

	Preliminary design goals	Achieved performance (Scan number 38, 10/24/86)
Mean pressure, MPa	15.0	15.1
Frequency, Hz	105.0	99.2
Average heater metal temperature, K	630.0	695.0
Average cooler metal temperature, K	315.0	350.0
Temperature ratio, $T_{hot}/T_{cold}$	2.0	1.99
Indicated or thermodynamic power, kW	30.7 (15.45/ cylinder)	
Indicated efficiency, percent	31.0	
Piston PV power, kW	28.8 (14.4/ cylinder)	24.9
Piston PV efficiency	29.1	15.9
Heat input, kW	99.0 (49.49/ cylinder)	156.7
Displacer amplitude, mm	8.97	9.6
Piston amplitude, mm	10.16	11.3
Displacer-piston Phase, deg	65.0	84.0
Compression space pressure amplitude, MPa	1.438	1.96
Piston-compression space pressure phase, deg	21.2	6.3

TABLE III. - SPACE STIRLING ENGINE (SSE)  
PRELIMINARY DESIGN OPERATING  
CHARACTERISTICS

Mean pressure, MPa . . . . .	18.5
Frequency, Hz . . . . .	90.0
Average heater metal temperature, K . . . . .	1050.0
Average cooler metal temperature, K . . . . .	525.0
Temperature ratio, $T_{hot}/T_{cold}$ . . . . .	2.0
Piston PPV power, kW . . . . .	37.7
Piston PV efficiency . . . . .	33.7
Heat input, kW . . . . .	112.0
Displacer amplitude, mm . . . . .	12.0
Piston amplitude, mm . . . . .	15.0
Displacer-piston phase, deg . . . . .	45.0
Compression space pressure amplitude, MPa . . . . .	2.03
Piston-compression space pressure phase, deg . . . . .	13.2

TABLE IV. - THERMODYNAMIC LOSS BREAKDOWN FOR ONE CYLINDER OF  
 SPACE POWER DEMONSTRATOR ENGINE (SPDE)  
 [Preliminary design calculations, 15.35 kW indicated  
 power/cylinder, 49.49 kW heat input/cylinder.]

Working space power losses	kW	Percent of indicated power or heat input
Hysteresis (expansion and compression spaces, heater, cooler, cooler-compression space connecting duct)	1.62	10.6
Leakage	0.36	2.3
Working fluid pumping		
Heater	0.67	---
Regenerator	.96	---
Cooler	.29	---
Cooler-compression space connection duct	.19	---
Total pumping	2.11	13.7
Loss due to heater and cooler gas-to-wall temperature difference	1.19	7.8
Working space thermal losses		
Conduction	1.86	3.8
Regenerator reheat or enthalpy flux	3.83	7.7
Appendix gap	1.33	2.7
Gas spring power losses (all three springs)		
Hysteresis	.73	4.8
Other (leakage, porting, etc.)	.69	4.5
Total gas spring losses	1.42	9.3

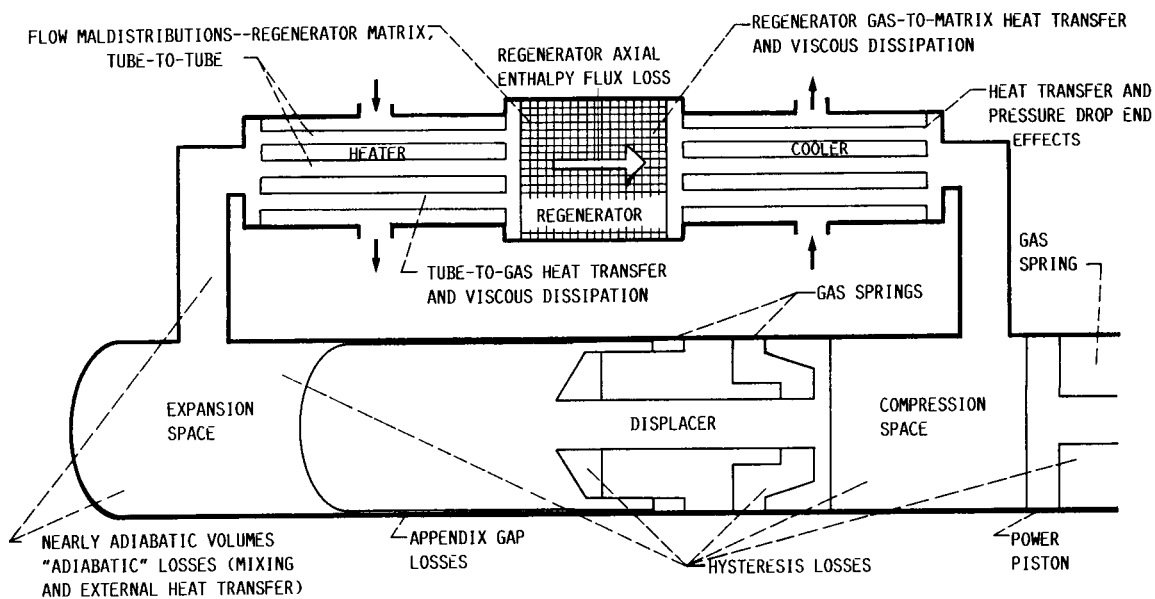


FIGURE 1. - STIRLING ENGINE SCHEMATIC WITH LOCATIONS OF HEAT TRANSFER AND FLUID FLOW PROBLEM AREAS.

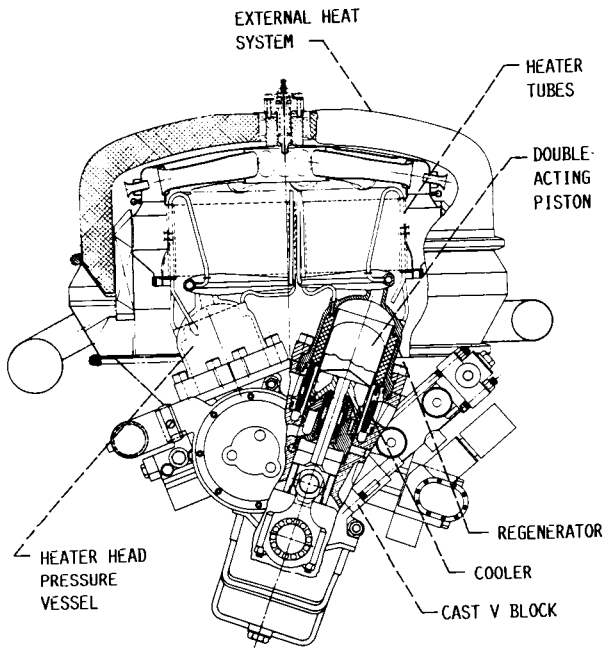
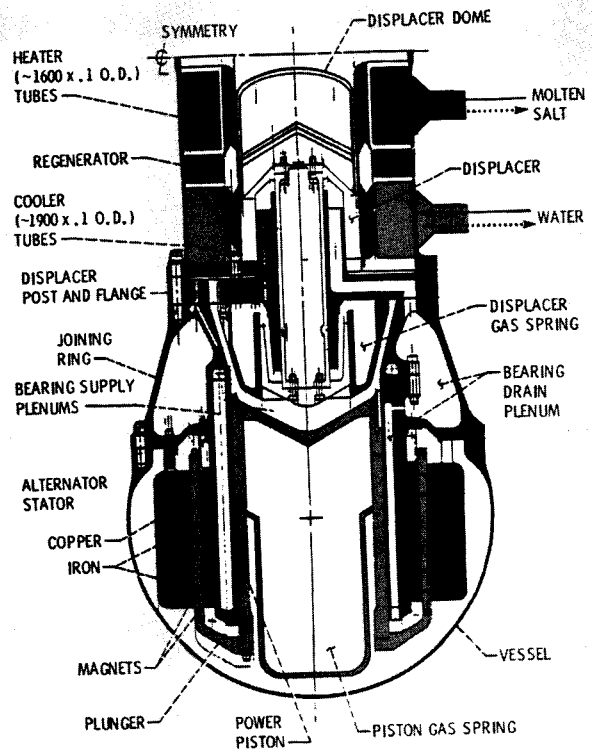


FIGURE 2. - MOD II CROSS SECTION.



CD-85-15398

FIGURE 3. - 25 kWe SPDE.

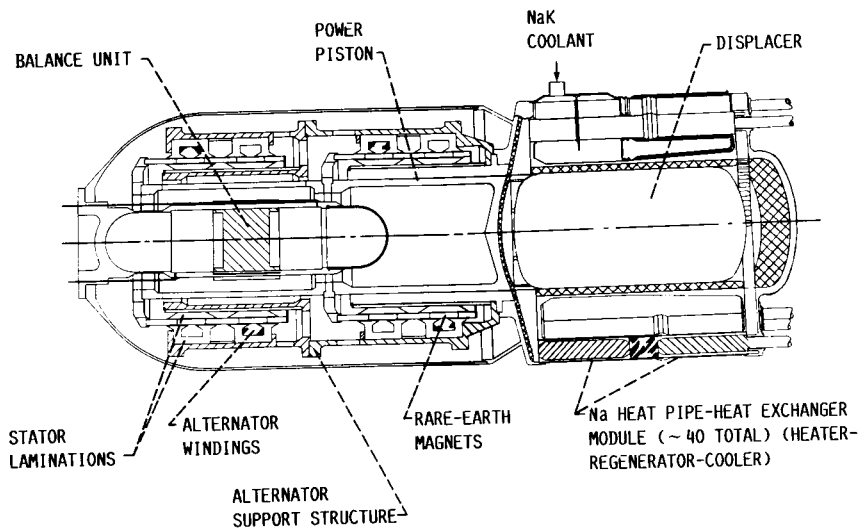


FIGURE 4. - STIRLING SPACE ENGINE, SSE.

ORIGINAL PAGE IS  
OF POOR QUALITY

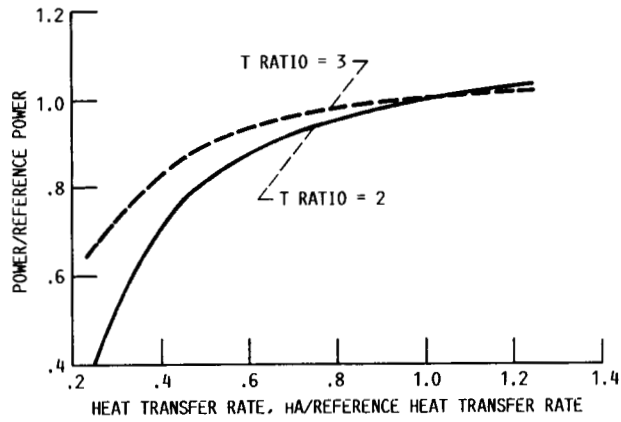


FIGURE 5. - SSE RELATIVE POWER AS A FUNCTION OF RELATIVE HEATER AND COOLER HEAT TRANSFER RATES.

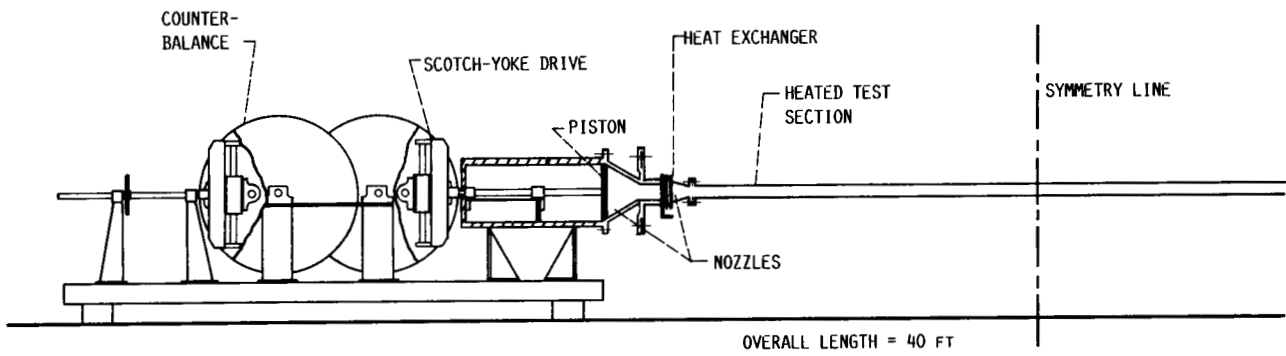


FIGURE 6. - SIDE VIEW OF THE OSCILLATING FLOW TEST RIG.

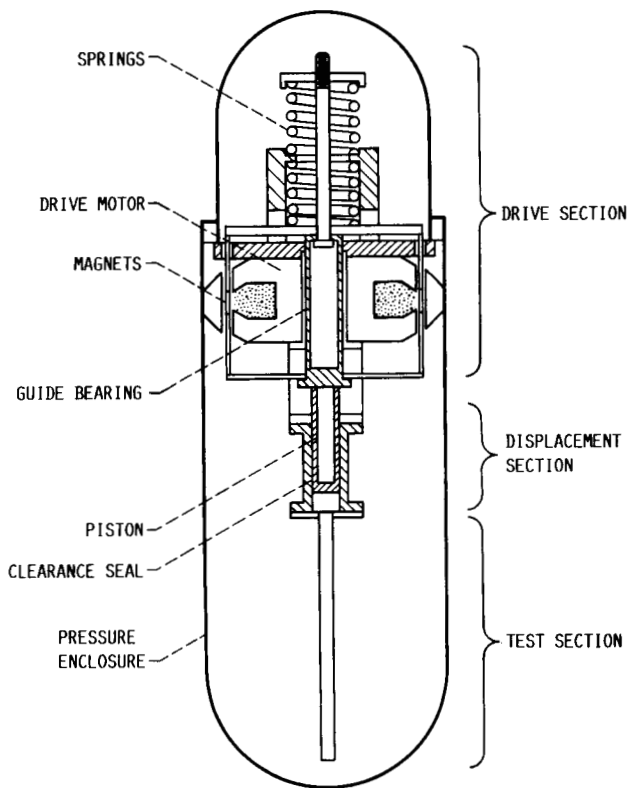


FIGURE 7. - SUNPOWER DESIGNED OSCILLATING FLOW TEST RIG.

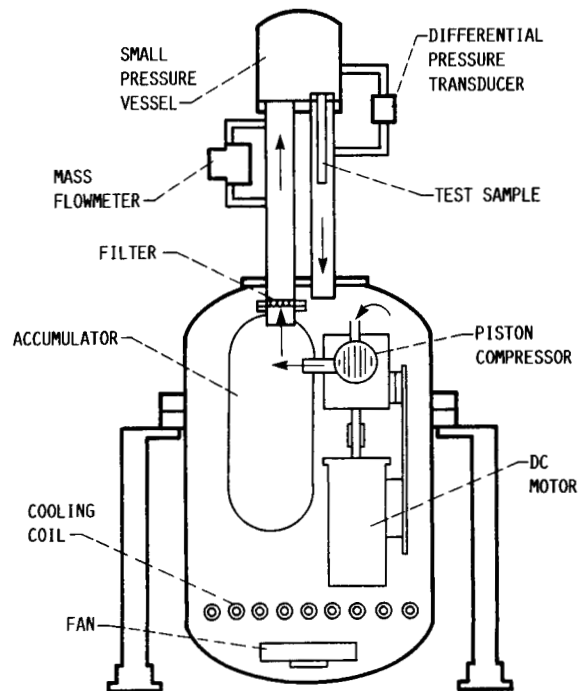


FIGURE 8. - STEADY FLOW TEST RIG.

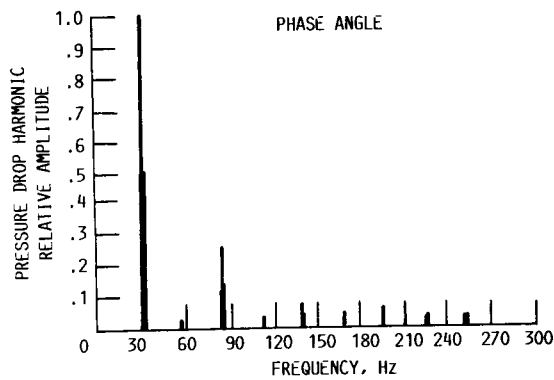
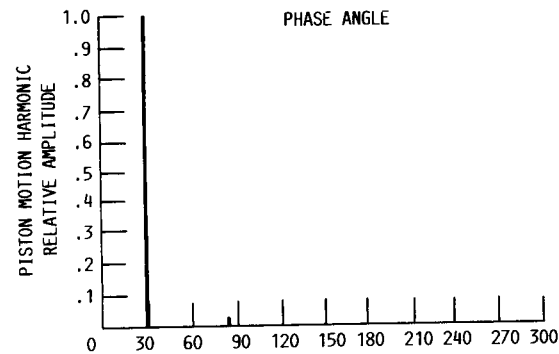
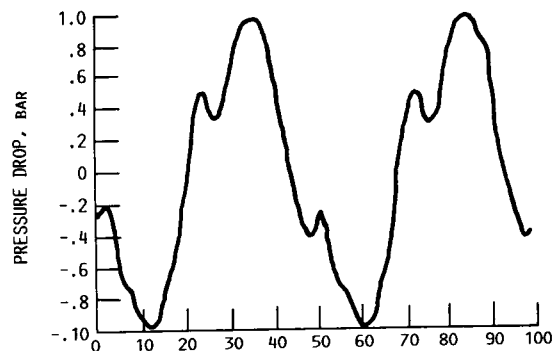
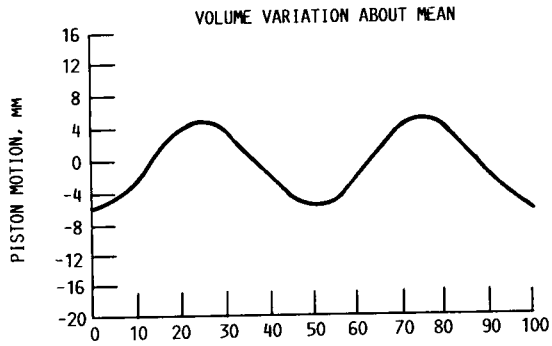


FIGURE 9. - OSCILLATING FLOW RIG DATA.

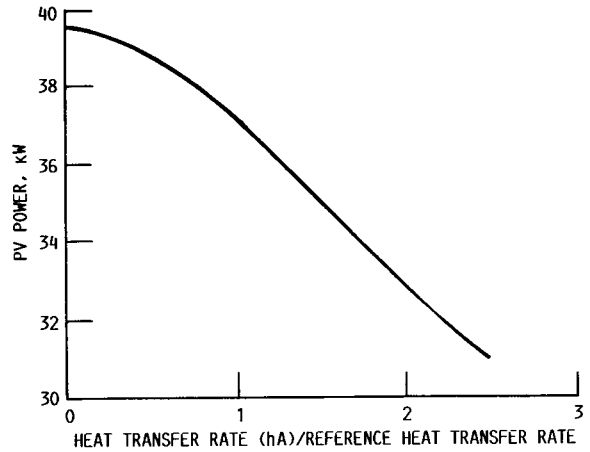


FIGURE 10. - SSE POWER AS A FUNCTION OF EXPANSION AND COMPRESSION SPACE HEAT TRANSFER RATES.

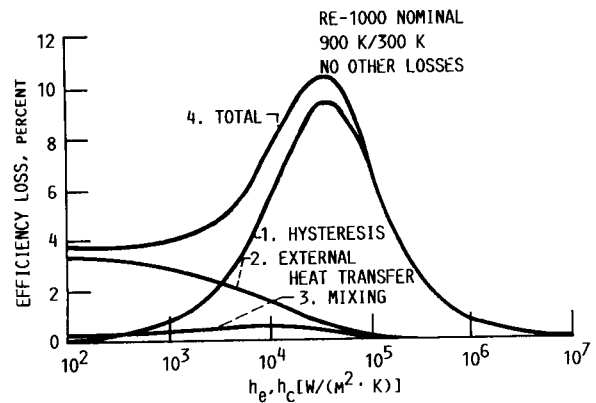


FIGURE 11. - LOSSES IN ENGINE WITH NONISOTHERMAL CYLINDERS.

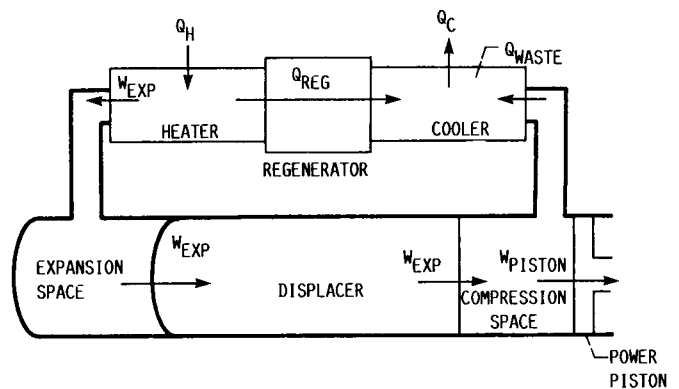
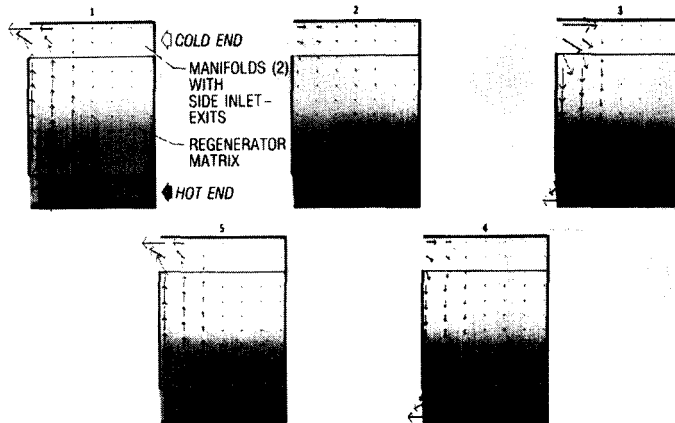


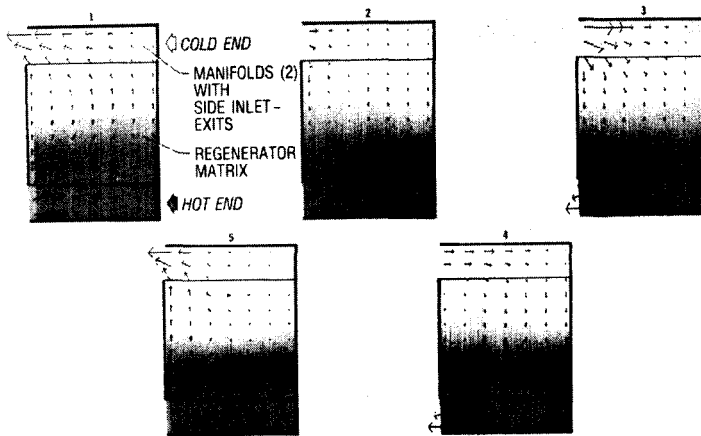
FIGURE 12. - INTEGRATED (OVER CYCLE) ENERGY FLUXES ACROSS COMPONENT BOUNDARIES.

ORIGINAL PAGE IS  
OF POOR QUALITY



FIVE PLOTS OF MASS FLUX PER UNIT AREA COMPUTED AT INTERVALS OF 1/5 CYCLE. READ CLOCKWISE. BASED ON SIMILAR GEOMETRY TO SUNPOWER 25 KW SPACE POWER ENGINE (HOWEVER, THIS ENGINE DOES NOT HAVE SIDE-INLET MANIFOLDS). CD-97-24088

FIGURE 13. - COMPUTED MASS FLOW RATE FOR SIDE-INLET-MANIFOLD REGENERATOR.



PLOTS OF MASS FLUX PER UNIT AREA WITH MATRIX FRICTION FACTOR INCREASED BY A FACTOR OF 50. CD-97-24089

FIGURE 14. - COMPUTED MASS FLOW RATE FOR SIDE-INLET-MANIFOLD REGENERATOR WITH INCREASED MATRIX FRICTION FACTOR.



# Report Documentation Page

1. Report No. NASA TM-100131	2. Government Accession No.	3. Recipient's Catalog No.	
4. Title and Subtitle Overview of Heat Transfer and Fluid Flow Problem Areas Encountered in Stirling Engine Modeling		5. Report Date February 1988	6. Performing Organization Code
		8. Performing Organization Report No. E-3680	
7. Author(s) Roy C. Tew, Jr.		10. Work Unit No. 506-41-31	
		11. Contract or Grant No.	
9. Performing Organization Name and Address National Aeronautics and Space Administration Lewis Research Center Cleveland, Ohio 44135-3191		13. Type of Report and Period Covered Technical Memorandum	
		14. Sponsoring Agency Code	
12. Sponsoring Agency Name and Address National Aeronautics and Space Administration Washington, D.C. 20546-0001			
15. Supplementary Notes A shortened version of this report was presented at the 1987 Winter Annual Meeting of the American Society of Mechanical Engineers, Boston, Massachusetts, December 14-16, 1987.			
16. Abstract NASA Lewis Research Center has been managing Stirling engine development programs for over a decade. In addition to contractual programs, this work has included in-house engine testing and development of engine computer models. Attempts to validate Stirling engine computer models with test data have demonstrated that engine thermodynamic losses need better characterization. Various Stirling engine thermodynamic losses and efforts that are underway to characterize these losses are discussed.			
17. Key Words (Suggested by Author(s)) Stirling engine; Heat engine; Stirling computer model; Stirling engine heat transfer; Stirling engine fluid flow		18. Distribution Statement Unclassified - unlimited STAR Category 85	
19. Security Classif. (of this report) Unclassified	20. Security Classif. (of this page) Unclassified	21. No of pages 22	22. Price* A02